IJCRT.ORG ISSN : 2320-2882

INTERNATIONAL JOURNAL OF CREATIVE RESEARCH THOUGHTS (IJCRT)

An International Open Access, Peer-reviewed, Refereed Journal

STUDY OF PRE-PROCESSING TECHNIQUES AND ATMOSPHERIC CORRECTION FOR A REMOTE SENSED IMAGE

Kavya Sathish
ECE Department
NMIT, Bangalore

Kushalatha M. R
ECE Department
NMIT, Bangalore

Tahera Zaiba Siddiqua
ECE Department
NMIT, Bangalore

Abstract: **Remote sensing is the acquisition of information about an object without making physical contact with it and it captures images of reasonably large areas. Regardless of instrumentation, picture acquisition is constantly enhanced by installing faster and more durable detectors, adding new cooling systems, and upgrading light sources. Nonetheless, there are a few considerations to address before beginning any sample's data processing (e.g., image compression, noise removal, removal of spiked points, background removal etc.). As a result, image pre-processing is virtually always necessary.**
In this paper, we perform atmospheric correction and pre-processing of a hyperspectral image (HSI). After applying the proposed techniques on Indian Pines, the SNR of the dataset has increased from 13.4264 to 23.7888 dB. After applying classification algorithms, we get 71.1823% as overall accuracy with kappa coefficient of 66.68% for BTC and 90.357% with kappa coefficient of 88.72% for KBTC. Except for calculation time, KBTC (Kernel Basic Thresholding Classifier) delivers the best performance in all criteria. There are substantial performance differences between the KBTC and the BTC (Basic Thresholding Classifier) algorithm.

Keywords—Indian Pines, Median, Gaussian, IARR, BTC, KBTC

I. INTRODUCTION

Remote sensing is a useful tool for gathering information about the earth's surface since it can take photos of a vast region. In the realm of remote sensing, hyperspectral imaging (HSI) data are crucial. It comprises not just spatial but also rich spectral information, unlike natural photographs. As a result, it's frequently utilized in urban planning, earth observation, agriculture, and food safety, among other applications.

The purpose of this paper is to demonstrate how to use some of the most prevalent options to fix the concerns listed above prior to image processing.

A hyperspectral image is a large set of data stored in pixels, each of which is closely linked to its neighbors. As a result, they include several data points. The application of traditional multivariate data analysis techniques to the analysis of hyperspectral data cubes (such as Multivariate Curve Resolution or PCA-Principal Component Analysis) made it possible to handle this volume of data and extract the relevant information, demonstrating broad application and success in obtaining the required data.

However, when it comes to data analysis, there is a fundamental issue that does not always get the attention it needs. The presence of erroneous data values (also known as dead pixels), non-informative background, outliers (observations that appear to be out of step with the rest of the dataset) obstructs subsequent identification, classification, and even quantification processes. A variety of factors can cause these unusual observations:

1) The instrument: The bulk of measurement systems employ diode array detectors or tunable filters. Zero values (dead pixels), odd spectrum readings (i.e., extreme values), or spiked spots in one wavelength can all be caused by a malfunction of one of the detector array's diodes.

2) The sample geometry: The sample geometry may differ significantly. Regardless, the photographs created are usually square in shape and feature both the exterior background and the sample's intriguing section.

3) Radiation: Different artefacts affect different spectroscopic techniques, as is well known. These artefacts might be formed by the sample's influence when irradiated, or by the spectral technique's behavior when irradiating the sample (for example, light scattering in Near Infrared Spectroscopy — NIR) (e.g., the fluorescence background in Raman spectroscopy). To ensure that any image processing tool or multivariate data analysis approach is used to its greatest potential, the images must first be pre-processed. The

applicability and performance of image pre-processing techniques and algorithms are influenced by the type of image measured, the device used, and the information intended to be retrieved from the analysis. The purpose of pre-processing is to get data that is free of contamination so that it can be processed later.

Fortunately, most hyperspectral sensor software packages include multiple picture pre-processing ('cleaning' phase) techniques. Choosing the optimal pre-processing technique or establishing objective criteria to address any of the issues listed is, however, a difficult undertaking. Before moving on to data processing, the purpose of this study is to present a comprehensive overview of the issues that occur in hyperspectral imaging. Simultaneously, we will discuss the advantages and disadvantages of the most common strategies for resolving those problems from the standpoint of practitioners. This study aims to shed some light on the process and provide a clear overview of the correct actions to take when pre-processing images before performing a full analysis. Throughout this manuscript, real samples with various challenges will be utilized to demonstrate the application of the various approaches proposed.

Various factors, however, can affect the image quality obtained throughout the HSI collection process. This could affect the accuracy of the image analysis. In order to produce a more accurate depiction of the original scene, picture rectification and restoration attempts to restore image data that has been damaged or deteriorated. Pre-processing is a phrase used to describe the procedure that occurs before the actual image analysis, which extracts information from a picture for a specific application. (1) Radiometric pre-processing to modify digital values for the influence of, say, a hazy atmosphere, and/or (2) Geometric pre-processing to align a picture with a map or some other images are two common pre-processing activities. The goal of pre-processing is to increase image quality so that we can better analyze it.

The primary goal of remote sensing has been to characterize the attributes of objects by detecting, registering, and analyzing the radiant flow that they emit or reflect. However, due to the presence of an extremely dynamic medium between the sensor and the earth surface, the mechanism for acquiring this radiation is not perfect. This atmosphere interacts with electromagnetic radiation, causing major changes in the target's incoming radiant flux. As a result, a greater emphasis on minimizing atmospheric influences on captured pictures through the use of atmospheric correction algorithms becomes necessary.

In this paper, we show how to pre-process an HSI for subsequent processing, including noise reduction, atmospheric correction, and dimensionality reduction. Following that, we use classification to assign a class label to each pixel in the HSI.

For HSI classification, we propose two non-linear kernel versions, BTC and KBTC. BTC is a sparsity-based linear classifier that uses the inner product as a similarity metric since hyperspectral data are linearly separable in feature space. In HSI classification, KBTC can be employed as a basic classifier. When the classes in a given data set are linearly non-separable, the suggested nonlinear sparsity-based method can obtain better classification results than linear sparsity-based methods.

II. Literature Survey

The paper written by Maider Vidal and Jose Manuel Amigo concludes that pre-processing of HSI's is a mandatory step [21]. Gustavo Camps-Valls explains that graph kernel is a powerful alternative to existing approaches for spatio-spectral remote sensing image classification [29]. The paper uses watershed algorithms Savitzky-Golay filtering which showed an increase of 0.51 in entropy [1]. The graph-based approach and gradient-ascent based approach are used to reduce computational complexities [2]. In the paper 'Noise Removal Based on Tensor Modeling for Hyperspectral Image Classification', noise parameters are estimated by using HYNPE algorithm. And for the denoising framework the multiple linear regression (MLR) based denoising method and tensor-based multiway Weiner filter are used. Salah Bourennane, Caroline Fossati and Tao Lin concluded that it is worth taking into account noise signal-dependency hypothesis for processing HYDICE and ROSIS HSIs [6]. In paper by Yicong Zhou, Jiangtao Peng, C L Philip Chen, they observed that the multiscale spatial WMF increases the neighboring pixel consistency and provides the rich and robust complementary [13].

The authors Guangchun Luo, Guangyi Chen, Ling Tian, Ke Qin and Shen-En Qian combine MNF/PCA with wavelet shrinkage, BM3D, VBM3D, BM4D, VBM4D, and NL-Means for denoising of HSI. Results show that MNF-based methods achieve higher SNR's than the PCA-based methods for reducing signal dependent noise in HSI data cubes. But for Gaussian white noise, PCA-based denoising methods have higher SNR's than the MNF-based methods [11]. The paper written by Sivert Bakken has tried dimensionality reduction methods such as PCA, MNF & JADE ICA on hyperspectral image. They concluded that MNF representation performed well on the Salinas scene dataset [8].

A number of experiments were performed in both real and simulated data conditions to illustrate the performance of the NAILRMA method for denoising of HSI in the paper written by Wei He, Hongyan Zhang, Liangpei Zhang, Huanfeng Shen. Here the high-SNR bands are effectively preserved by noise adjusted iteration strategy and the low-SNR bands are denoised. The randomized singular value decomposition method is then used to solve the NAILRMA optimization problem [14]. Craig Rodarmel and Jie Shan used HYDICE and AVIRIS datasets for the study in which they used principal composition analysis approach and examined the information contents of the principal component image bands. They concluded that only the first few bands contain significant information and yield about 70% correct classification rate [12].

The paper by Rajesh Gogineni and Ashvini Chaturvedi discusses the recent progress in the classification of HSI's in the aspects of Kernel-based methods, supervised and unsupervised classifiers, classification based on sparse representation, and spectral-spatial classification [3]. In this paper 'Edge Detection with a pre-processing Approach', multilevel image segmentation is performed then a standard edge detection method is applied on this image segmentation. The authors have concluded that edge detection with the pre-processing approach provides better performance than other standard methods [19].

Behzad Nazarbakhsh and Azizah Abd Manaf carried out the classification using eigen distances values and comparing values of the dataset. The resultant tests from the data set yielded the following results: true acceptance rate at 91.30 % and false acceptance rate at 33.33 %. This shows that the proposed image pre-processing framework improves the recognition accuracy as compared to not applying it [20]. By applying Fusion-FCN on multispectral LiDAR, overall accuracy of 80.7% was obtained. The paper written by Seyyid Ahmed Medjahed and Mohammed Ouali shows that the performance and the effectiveness of simulated anealing approach on Pavia University gave satisfactory results compared to filter methods and other hyperspectral classifiers [4].

Authors Sukumuran Minu, Amba Shetty and Cecile Gomez concluded that ATCOR performs better than RT from 2000nm to 2350nm, while RT performs better than ATCOR in 400nm to 1050nm in terms of spectral similarity in their paper [5]. The paper by Chinsu Lin, Tsogta and Chang examines the effects of pansharpening and atmospheric correction on LULC classification. Here the LULC classification accuracy using PB-MLC and OB-SVM is 82% and 89% respectively [15]. On MERIS FR and OLI scenes, the performance of OPERA with and without the SIMEC adjacency correction was evaluated and Sterckx, Knaeps and Reusen concluded that the effect of SIMEC on the final reflectance depends on the AC algorithm applied [16].

By using MH prediction on AVIRIS dataset in the paper by Chen, Tramel, Prasad and Fowler, classification accuracy has been increased significantly [17]. The main difficulty of HSI classification lies in the few labelled samples versus the high dimensional features. The paper written by Rongrong Ji, Yue Gao, Richang Hong, Qiong Liu, Dacheng Tao and Xuelong Li shows on how to solve this problem. They have conducted experiments on four datasets to evaluate the effectiveness and efficiency. The proposed method achieves performance gains of 15.04%, 33.84%, 6.40%, 15.71% [18].

For HSI classification, Qishuo Gao, Samsung Lim and Xiuping Jia used CNN. The proposed method not only takes advantage of enhanced feature extraction from CNNs, but also fully exploits the spectral and spatial information jointly. The effectiveness of the proposed method is tested with three benchmark data sets, and the results show that the CNN-based multi-feature learning framework improves the classification accuracy significantly [7]. The paper written by Mehmet Altan Toksöz and ˙Ilkay Ulusoy explains how BTC is performed [9].

Mehmet Altan Toksöz in his paper basic thresholding classifier explains the working of KBTC [10]. In paper written by Jun Li, José M. Bioucas-Dias, and Antonio Plaza, they proposed a new framework for spectral–spatial hyperspectral classification using belief propagation which suited well to problems with very few training samples [22]. In the paper written by Gabriel Martin and Antonio Plaza, they concluded that the proposed method is accurate in the task of identifying end members from complicated scenes [23]. In the paper written by Sowmya V Kavitha Balakrishnan and KP Soman, they used an actual hyperspectral dataset to test the approach. The results of the experiments showed that using a spatial pre-processing technique on the hyperspectral band, enhanced image quality and produced better within-class variability, resulting in an increase in classification accuracy [24].

Xuefeng Liu, Salah Bourennane and Caroline Fossati in their paper concluded that the PARAFAC model is a better denoising method, according to the results, because the variance of the HSI denoised by it is closer to the CRLB than the other methods evaluated [25]. Daniel Scheffler and Pierre Karrasch used data from the EO-1 Hyperion instrument in their study. They found that some correction approaches have little influence on image striping [26]. Qiangqiang Yuan, Liangpei Zhang and Huanfeng Shen in their paper showed that the suggested method can successfully realise the spectral-spatial adaptive mechanism in the denoising process, resulting in superior denoising results for numerous experiments [27].

In their paper, Behnood Rasti, Johannes R. Sveinsson, Magnus O. Ulfarsson and Jon Atli Benediktsson offer a 3D wavelet-based denoising approach for hyperspectral pictures in this work. They employed a 3D overcomplete wavelet dictionary to do sparse analysis regularisation. The iterative Chambolle algorithm is used to solve the minimization issue. In terms of Peak Signal to Noise Ratio, the simulation results suggest that the 3D vocabulary surpasses the 2D dictionary (PSNR). Denosing hyperspectral cubes is anticipated to improve hyperspectral data classification accuracy by enhancing spectral profiles (or features) that can be used to distinguish across information classes [28].

III. PROPOSED MODEL

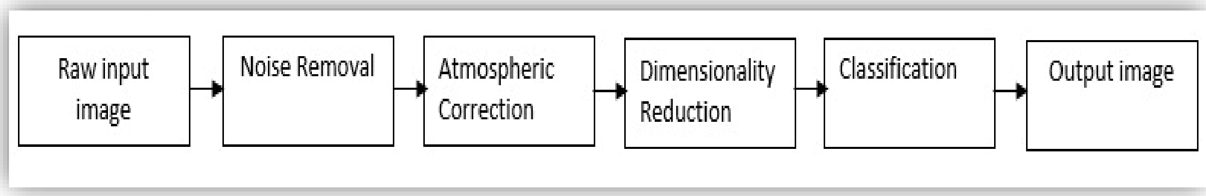

Fig 1: Block Diagram of the proposed model

A. Noise Removal:

Image de-noising is an important image pre-processing procedure that can be used alone or as part of a larger process. De-noising an image or a piece of data can be done in a variety of ways. A decent photo denoising model should reduce noise as completely as feasible while keeping edges as much as possible. There were two types of models: linear and non-linear. Here we are using Gaussian and Median filter for denoising.

- *Gaussian Filter*

A linear filter is a Gaussian filter. It is most commonly used to blur images or minimize noise. You can use them for "unsharp masking" (edge detection) if you combine two of them and subtract. Also, the Gaussian filter blurs edges and reduces contrast.

- *Median Filter*

The Median filter is a non-linear filter that is frequently used to minimize image noise. It reduces noise while maintaining sharp edges. Because multiplication and adding is probably faster than sorting, a Gaussian filter has the advantage of being faster than a median filter.

B. Atmospheric Correction:

Solar radiation scattered from the Earth's surface interacts with the atmosphere before reaching any space-based or airborne remote sensing sensor. Solar radiation scattered from the Earth's surface interacts with the atmosphere before reaching any space-based or airborne remote sensing sensor. The actual brightness reported at any particular spot on the ground is affected by air interaction (mostly absorption and scattering). The degree of absorption and scattering, however, varies geographically and temporally depending on the composition and concentration of various atmospheric constituents. In portions of the EMR spectrum such as 0.9, 1.1, 1.4, and 1.9 m, remote sensing sensors are nearly opaque. As a result, transmission windows are defined as areas with no major absorption features. Remote sensing sensors take advantage of these transmission widows. However, these are subject to atmospheric effects that must be appropriately addressed in order to improve understanding. In this case, any further hyperspectral image pre-processing and appropriate interpretation require atmospheric correction.

Water vapor, molecular gases and aerosol particles are present in all atmospheric layers, and information on these elements can be retrieved from hyperspectral imaging using specially built algorithms. These techniques can then be utilized to characterize the atmosphere in a reliable radioactive transfer programme, allowing for the estimation of spectral ground reflectance and ground-cover classification.

To remove the effects of atmosphere, we are performing atmospheric correction using the IARR. The IAR method normalizes images to a scene average spectrum. When comparing radiance and reflectance spectra, the IAR Reflectance approach provides a simpler spectral curve to read than alternative correcting methods.

C. Spectral Dimensionality Reduction:

Crop analysis, geological mapping, mineral prospecting, and other concerns can all benefit from hyperspectral imaging. Dimensionality reduction has become an important feature of machine learning due to the fact that the data contains a large number of bands. It is frequently used as a pre-processing step in the solution of machine learning tasks like classification and clustering. The number of dimensions or features will, in general, influence the accuracy of any classification and clustering process.

The number of dimensions in the dataset is reduced using dimensionality reduction techniques, allowing classifiers to generate detailed model at a minimal cost of computation. As a result, Dimensionality Reduction (DR) has gained in popularity as a way to increase pixel categorization accuracy in Hyperspectral Images (HSI).

Dimensionality reduction is the process of lowering the dataset's dimensions or features. There are two techniques to minimise the dataset's dimensionality. They are:

- Selection of Features
- Extraction of Features

The process of selecting the dimensions of dataset features that contribute to ML tasks like as classification, clustering, and so on is known as feature selection. This can be accomplished by employing several techniques such as correlation analysis, univariate analysis, and so on.

The technique of identifying new features by identifying and/or merging existing features to reduce feature map whilst accurately and comprehensively characterizing the data set without damaging info is known as feature extraction.

In our paper, we are performing feature extraction using two approaches, namely- PCA and MNF.

PCA- Principal Component Analysis

PCA (Principal Component Analysis) is a commonly used method that dates back to the beginning of the twentieth century in a variety of fields. It has been renamed multiple times and is known by various distinct names. It's also known as Karhunen-Loeve transformation or simply PCA in the hyperspectral imaging sector. The approach remains the same in essence regardless of the algorithm's origin. By identifying the eigenvalues of C, the PCA transformation attempts to diagonalize the sample covariance matrix C.

$$\det(C - \sigma^2 I) = 0$$

Given the full rank of the C matrix, which means no eigenvalue can be zero, the eigenvalues 2 obtained will indicate the variance for each eigenvector. In addition, the main direction in which the spectral correlation is reduced is given by

$$C\, v_j = \sigma^2 v_j$$

The j^{th} eigenvector corresponds to the j^{th} eigen value, and v_j is an eigen vector of unit length. The following relationship can be established if all the eigenvalues were ordered in a diagonal matrix D with the highest eigen value first and the smallest eigen value last as:

$$\Longrightarrow \quad CV = VD \qquad C = VDV^T$$

Following the fact that V is an orthogonal unitary matrix, the associated eigenvectors v_j are also arranged in descending order, as with the D matrix. As a result, the original projection is transformed into an orthogonal basis, where the bands are uncorrelated and arranged according to the variance of the original data:

$$Z = V^T X$$

The principal component data matrix translation from the original coordinate space to an orthogonal coordinate space is represented by Z. With K as the whole dimensional space, you would choose the k <= K biggest associated eigen vectors and eigen values to execute the desired dimensionality reduction, i.e., represent the original data using fewer samples or variables. Ideally, the inverse transformation would return the original data with less noise.

Maximum Noise Fraction (MNF)

Maximum noise fraction, also known as minimum noise fraction, was first described in and has since been used in a variety of hyperspectral and multispectral image analysis approaches, with the basic idea having been developed many times since then. MNF's goal is to sort the components based on noise, or rather estimated noise, rather than variance, like PCA does. It is usual to assume that the signal covariance and the noise covariance are independent from the outset:

$$\Sigma = \Sigma_s + \Sigma_n$$

where Σ_s and Σ_n are the covariances of the actual desired signal and noise, respectively, and Σ signifies the overall covariance of the samples.

Because the noise cannot be known in advance, it must be calculated. The key distinction between MNF methods is how this estimation is achieved. There are numerous approaches to performing this estimation. One of the original ones is mentioned below. Green calculates noise under the premise that all of the data, or at least a piece of it, is from a homogenous location. As a result, we can calculate the difference between signals.

$$X_n = [\, x_1 - x_2,\ x_2 - x_3,\ \ldots,\ x_{N-1} - x_N \,]$$

The noise's covariance and singular value decomposition can be obtained in the following manner:

$$C_n = X_n^T X_n \qquad C_n = \mathrm{svd}(C_n) = U_n S_n V_n^T$$

The noise data must be decorrelated, commonly known as whitening. The following steps can be used to whiten or make the covariance uncorrelated and of unit variance:

$$X_w = X U_n S_n^{-1/2} \quad X_w = \mathrm{svd}(X_w) = U_w S_w V_w^T$$

D. Classification:

A three-dimensional data cube including two-dimensional spatial and one-dimensional spectral information is called a hyperspectral image (spectral-bands). Although the spectral bands have very small wavelengths, image properties such as Land cover features and shape features disclose the disparity and relationship among neighbouring pixels from various angles at a trustworthy wavelength.

In the field of remote sensing, the phrase classification refers to the process of allocating individual pixels to a set of classes. The classification phase's outcome is the classification map. Based on the availability of training data, classification techniques can be classified into two categories: supervised and unsupervised classifiers. Supervised approaches classify incoming data for each class using a set of typical samples known as training samples. Hyperspectral image classification has many flaws, including high dimensionality, limited or imbalanced training sets, spectral variability, and mixing pixels.

This thesis proposes the BTC (Basic Thresholding Classifier), a sparsity-based technique for classification applications (such as face recognition, hyperspectral image classification, and so on). It has the ability to instantly detect test samples and classify them with high accuracy. BTC is a linear classifier that operates on the assumption that samples from different classes in a dataset are linearly separable. In practise, however, those samples may not be linearly separable. We also offer the KBTC (kernel basic thresholding classifier), a non-linear kernel variation of the BTC approach, in this context. KBTC can produce good results when the input samples are linearly non-separable.

In both ideas, we provide sufficient identification criteria (SICs) for Basic Thresholding Classifier and Kernel Basic Thresholding Classifier to identify any test sample in a dictionary's range space. We use SICs to create parameter estimate algorithms that don't require cross validation. Individual classifier outputs are fused to improve classification outcomes in both the Basic Thresholding Classifier and Kernel Basic Thresholding Classifier methods. In the case of face recognition, for example, the residuals from various random projectors are combined.

Fusion is accomplished for applications like HSI classification by combining spatial information and smoothing the residual maps. On publicly available face and HS datasets, our proposal surpasses well-known SVM (support vector machines) based techniques, MLR (multinomial logistic regression) based methods, and sparsity-based approaches like l1-minimization and SOMP (simultaneous orthogonal matching pursuit) in terms of classification accuracy and computational cost.

IV. Experimental Results

A. Dataset

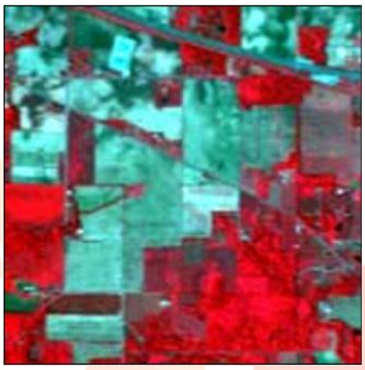

Fig. 2. Indian Pines dataset

With 145x145 pixels and 224 spectral reflectance bands in the wavelength range of 0.4–2.5 10(-6) metres, the AVIRIS sensor photographed this image above the Indian Pines test site in northwestern Indiana. This is a little part of a larger scene. Farmland makes up two-thirds of the scene in Indian Pines, with woodland or other natural perennial vegetation making up the other one-third. There are two major dual-lane highways, a rail line, as well as some low-density housing, other man-made structures, and minor roads. Some of the crops, such as maize and soybeans, are still in the early stages of development, with less than 5% coverage, since the snapshot was taken in June.

B. Median filter-Result

The median filter checks each pixel in the image individually and compares it to its neighbours to see if it is representative of the area. The median of those values is used instead of just replacing the pixel value with the mean of neighbouring pixel values. The median is calculated by numerically ranking all of the pixel values in the immediate vicinity and then substituting the middle pixel value for the pixel in issue (If the number of pixels in the neighbourhood under consideration is even, the average of the two middle pixel values is utilised).

Here we are extracting and displaying the individual red, green, blue channels and then using median filter to remove the noise.

The SNR of original image is 13.4264 dB and SNR of denoised image using median filter is 13.5113 dB.

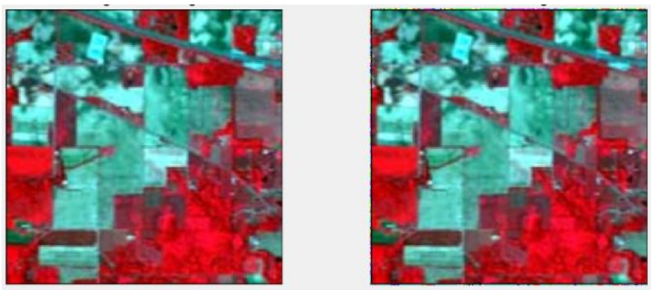

Fig.3. Image after Median filter

C. Gaussian Filter- Result

Smoothing photos with Gaussian filtering is more effective. Its origins can be traced back to the human visual perception system. In the human visual perception system, it has been discovered. When neurons analyse visual images, they form a similar filter, according to research.

The hyperspectral image on the left has been smoothed with a Gaussian filter and displayed on the left.

SNR of denoised image using gaussian filter is 14.0455 dB.

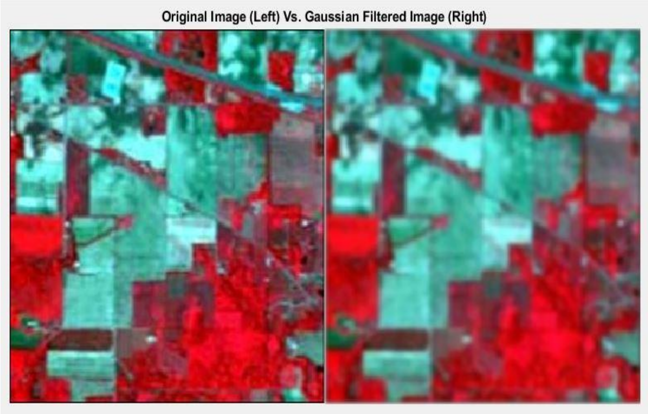

Fig. 4. Gaussian filter output

D. Atmospheric correction- Result

We use IAR Reflectance Correction (Internal Average Relative Reflectance) to normalize images to a scene-average spectrum. This is particularly useful for translating hyperspectral data to relative reflectance when there are no ground measurements and only a few details are known about the scene. The reference spectrum is made by splitting the average spectrum of the entire scene into the spectrum for each pixel in the image. We get 13.8011 dB as the SNR after atmospheric correction.

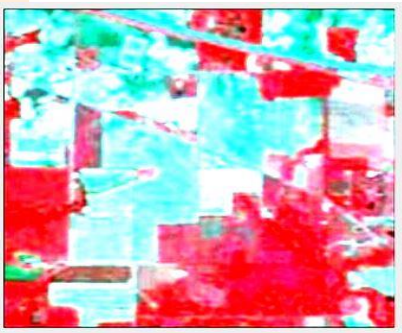

Fig.5. Image free from atmospheric effects

E. PCA- Result

Inevitably, decreasing the number of variables in a data set affects accuracy; therefore, the solution to dimensionality reduction is to give up some accuracy in exchange for greater simplicity, as smaller data sets are easier to grasp and interpret. In a word, PCA's purpose is to keep as much information as feasible while reducing the number of variables in a data set.

The function 'hyperpca' computes the requested number of main components from the hyperspectral data cube's spectral bands. The function creates a new data cube with the principal component bands in it. The resulting data cube has the same number of spectral bands as the number of provided principal components ('numComponents'). The stated number of primary components must be smaller than the number of spectral bands in the hyperspectral data cube to achieve spectral dimensionality reduction.

After applying PCA the SNR increases to 17.9979 dB.

Fig.6. I principal component band after applying PCA

F. MNF- Result

It converts a noisy data cube into output channel images with constantly increasing noise levels, implying that the image quality of the MNF output images is steadily deteriorating.

The 'hypermnf' function uses the maximum noise fraction (MNF) transform to compute the provided number of principal component bands (numComponents). The given number of primary components must be smaller than the number of spectral bands in the input data cube to achieve spectral dimensionality reduction.

The SNR has increased to 20.4616 dB after applying MNF.

Fig.7. I principal component band after applying MNF

G. Classification

Performance Indexes:

The following are the performance indices that were used in this paper.

- Overall Accuracy (OA): It's the percentage of pixels in all test samples that have been correctly classified.
- Average Accuracy (AA): The average of individual class accuracies gives this figure.
- k Coefficient: It is a metric that assesses the degree of consistency.

1. BTC- Result

- Overall Accuracy=71.1823%
- Average Accuracy=76.6761%
- K=66.6833%

Fig.7. Classification on BTC(71.1823%)

2. KBTC- Result

- Overall Accuracy=90.357%
- Average Accuracy=92.7976%
- K=88.7264%

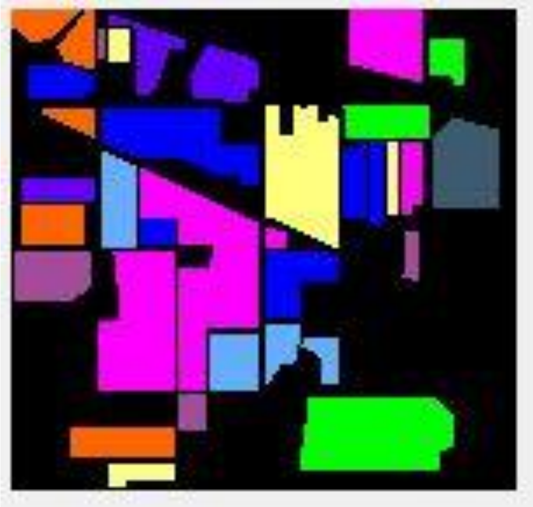

Fig.8. Classification on KBTC(90.357%)

Metric	BTC (%)	KBTC (%)
Overall Accuracy (OA)	71.1823	90.357
Average Accuracy (AA)	76.6761	92.7976
k coefficient	66.6833	88.7264

Table 1. Comparison between BTC and KBTC

V. Conclusion and Future Scope

Noise Removal using Median and Gaussian filter is done and the SNR have been calculated. Using Gaussian filter gave more SNR value than using Median filter. We have also reduced the spectral dimensionality of the data cube by using PCA and MNF methods. By doing this the SNR value have improved when compared to the SNR value of denoised image. We can observe that after applying MNF technique the SNR value is higher than in PCA technique. We can notice that SNR of the atmospherically corrected image has increased.

After applying the best suited techniques (denoised using Gaussian filter, reduced dimension by MNF and applied IARR for atmospheric correction) on Indian Pines, the SNR of the dataset has increased from 13.4264 to 23.7888 dB.

In this study, we used a nonlinear kernel variation of the previously disclosed BT classification algorithm. In tests where the samples of the classes are linearly non-separable, the suggested method outperforms the linear variant.

Except for calculation time, KBTC (Kernel Basic Thresholding Classifier) delivers the best performance in all criteria. The KBTC and BTC (Basic Thresholding Classifier) algorithms have significant performance differences.

As the real-world data in the feature space is extremely varied, we want to evaluate the suggested technique under other kernel learning frameworks in the future.

References

[1] Yu-hang Li, Xin Tan, Wei Zhang, Qing-bin Jiao, Yu-xing Xu, Hui Li, Yubo Zou, Lin Yang, and Yuan-peng Fang, *"Research and Application of Several Key Techniques in Hyperspectral Image Preprocessing",* 2021

[2] Subhashree Subudhi, Ram Narayan Patro, Pradyut Kumar Biswal, Fabio Dell'Acqua, "*Superpixel-Based Singular Spectrum Analysis for Effective Spatial-Spectral Feature Extraction*", 2021

[3] Rajesh Gogineni and Ashvini Chaturvedi, "*Hyperspectral Image Classification*", 2019

[4] Seyyid Ahmed Medjahed, Mohammed Ouali, "*Band selection based on optimization approach for hyperspectral image classification"*, 2018

[5] Sukumaran Minu, Amba Shetty, Cecile Gomez, "*Hybrid atmospheric correction algorithms and evaluation on VNIR/SWIR Hyperion satellite data for soil organic carbon prediction"*, 2018

[6] Salah Bourennane, Caroline Fossati and Tao Lin, "*Noise Removal Based on Tensor Modeling for Hyperspectral Image Classification*", 2018

[7] Qishuo Gao, Samsung Lim and Xiuping Jia, "*Hyperspectral Image Classification Using Convolutional Neural Networks and Multiple Feature Learning*", 2018

[8] Sivert Bakken, "*Dimensionality Reduction and Target Detection in Hyperspectral Remote Sensing*", 2018

[9] Mehmet Altan Toksöz, Student Member, IEEE, and ˙Ilkay Ulusoy, "*Hyperspectral Image Classification via Kernel Basic Thresholding Classifier*", 2017

[10] Toksöz, Mehmet Altan, "*Basic Threshold Classification*", 2016

[11] Guangchun Luo, Guangyi Chen, Ling Tian, Ke Qin and Shen-En Qian, "*Minimum Noise Fraction versus Principal Component Analysis as a Preprocessing Step for Hyperspectral Imagery Denoising*", 2016

[12] Craig Rodarmel and Jie Shan, "*Principal Component Analysis for Hyperspectral Image Classification*", 2015

[13] Yicong Zhou, Jiangtao Peng, C L Philip Chen," Dimension *Reduction Using Spatial and Spectral Regularized Local Discriminant Embedding for Hyperspectral Image Classification*", 2015

[14] Wei He, Hongyan Zhang, Liangpei Zhang, Huanfeng Shen, "*Hyperspectral Image Denoising via Noise-Adjusted Iterative Low-Rank Matrix Approximation*", 2015

[15] Chinsu Lin, Chao-ChengWu, Khongor Tsogta, Yen-Chieh Ouyang and Chein-I Chang, "*Effects of atmospheric correction and pansharpening on LULC classification accuracy using WorldView-2 imagery*", 2015

[16] Sindy Sterckx, Els Knaeps, Stefan Adriaensen, Ils Reusen, "*Opera: An Atmospheric Correction for Land and Water*", 2015

[17] Chen Chen, Wei Li, Eric W. Tramel, Minshan Cui, Saurabh Prasad and James E. Fowler, "*Spectral–Spatial Preprocessing Using Multihypothesis Prediction for Noise-Robust Hyperspectral Image Classification*", 2014

[18] Rongrong Ji, Yue Gao, Richang Hong, Qiong Liu, Dacheng Tao, Xuelong Li, "*Spectral-Spatial Constraint Hyperspectral Image Classification*", 2014

[19] Mohamed Abo-Zahhad, Reda Ragab Gharieb, Sabah M. Ahmed and Ahmed Abd El-Baset Donkol, "*Edge Detection with a Preprocessing Approach*", 2014

[20] Behzad Nazarbakhsh and Azizah Abd Manaf, "*Image Pre-processing Techniques for Enhancing the Performance of Real-Time Face Recognition System Using PCA",* 2014

[21] Maider Vidal, Jose Manuel Amigo, "*Pre-processing of hyperspectral images. Essential steps before image analysis ",* 2012

[22] J. Li, J. Bioucas-Dias, and A. Plaza, *"Spectral–spatial hyperspectral image segmentation using subspace multinomial logistic regression and Markov random fields,"* 2012

[23] Gabriel Martin, Antonio Plaza, "*Spatial-spectral pre-processing prior to endmember identification and unmixing of remotely sensed hyperspectral data",* 2012

[24] Sowmya V Kavitha Balakrishnan and KP Soman, "*Spatial preprocessing for improved sparsity based hyperspectral image classification*", 2012

[25] Xuefeng Liu, Salah Bourennane and Caroline Fossati, "*Denoising of hyperspectral images using the PARAFAC model and statistical performance analysis*", 2012

[26] Daniel Scheffler and Pierre Karrasch, "*Preprocessing of hyperspectral images: a comparative study of destriping algorithms for EO1-hyperion*", 2012

[27] Qiangqiang Yuan, Liangpei Zhang and Huanfeng Shen, "*Hyperspectral Image Denoising Employing a Spectral–Spatial Adaptive Total Variation Model*", 2012

[28] Behnood Rasti, Johannes R. Sveinsson, Magnus O. Ulfarsson and Jon Atli Benediktsson, "*Hyperspectral image denoising using 3D wavelets*", 2012

[29] Gustavo Camps-Valls, "*Spatio-Spectral Remote Sensing Image Classification with Graph Kernels*", 2010